

# The mitochondrial phylogeny of land plants shows support for Setaphyta under composition-heterogeneous substitution models

Filipe Sousa<sup>Corresp. 1</sup>, Peter Civiň<sup>1, 2, 3</sup>, João Brazão<sup>1</sup>, Peter Foster<sup>4</sup>, Cymon Cox<sup>Corresp. 1</sup>

<sup>1</sup> Centro de Ciências do Mar, Universidade do Algarve, Faro, Portugal

<sup>2</sup> INRA, Université d'Auvergne (Clermont-Ferrand I), Clermont-Ferrand, France

<sup>3</sup> Manchester Institute of Biotechnology, School of Earth and Environmental Sciences, University of Manchester, Manchester, United Kingdom

<sup>4</sup> Department of Life Sciences, Natural History Museum, London, United Kingdom

Corresponding Authors: Filipe Sousa, Cymon Cox  
Email address: fpsousa@ualg.pt, cymon@ualg.pt

Congruence among analyses of plant genomic data partitions (nuclear, chloroplast and mitochondrial) is a strong indicator of accuracy in plant molecular phylogenetics. Recent analyses of both nuclear and chloroplast genome data of land plants (embryophytes) have, controversially, been shown to support monophyly of both bryophytes (mosses, liverworts, and hornworts) and tracheophytes (lycopods, ferns, and seed plants), with mosses and liverworts forming the clade Setaphyta. However, relationships inferred from mitochondria are incongruent with these results, and typically indicate paraphyly of bryophytes with liverworts alone resolved as the earliest-branching land plant group. Here, we reconstruct the mitochondrial land plant phylogeny from a newly compiled data set. When among-lineage composition heterogeneity is accounted for in analyses of codon-degenerate nucleotide and amino acid data, the clade Setaphyta is recovered with high support, and hornworts are supported as the earliest-branching lineage of land plants. These new mitochondrial analyses demonstrate partial congruence with current hypotheses based on nuclear and chloroplast genome data, and provide further incentive for revision of how plants arose on land.

1 **The mitochondrial phylogeny of land plants shows**  
2 **support for Setaphyta under composition-**  
3 **heterogeneous substitution models**

4

5

6 Filipe de Sousa<sup>1</sup>, Peter Civián<sup>1,2,3</sup>, João Brazão<sup>1</sup>, Peter G. Foster<sup>4</sup>, Cymon J. Cox<sup>1\*</sup>

7

8

9 <sup>1</sup>Centro de Ciências do Mar, Universidade do Algarve, Gambelas, 8005-319 Faro, Portugal

10

11 <sup>2</sup>Manchester Institute of Biotechnology, School of Earth and Environmental Sciences, University  
12 of Manchester, Williamson Building, Manchester M13 9PL, United Kingdom

13

14 <sup>3</sup>INRA-Université Clermont-Auvergne, UMR 1095 GDEC, Clermont-Ferrand, France

15

16 <sup>4</sup>Department of Life Sciences, Natural History Museum, London SW7 5BD, United Kingdom

17

18 Corresponding Author: Cymon J. Cox<sup>1</sup>

19 <sup>1</sup>Centro de Ciências do Mar, Universidade do Algarve, Gambelas, 8005-319 Faro, Portugal

20 Email address: cymon.cox@googlemail.com

21

22

23

24

25

26

27

28

29

30

31

32

33

34

35

36

37

38

39

40

41

42

43

44

## **Abstract**

Congruence among analyses of plant genomic data partitions (nuclear, chloroplast and mitochondrial) is a strong indicator of accuracy in plant molecular phylogenetics. Recent analyses of both nuclear and chloroplast genome data of land plants (embryophytes) have, controversially, been shown to support monophyly of both bryophytes (mosses, liverworts, and hornworts) and tracheophytes (lycopods, ferns, and seed plants), with mosses and liverworts forming the clade Setaphyta. However, relationships inferred from mitochondria are incongruent with these results, and typically indicate paraphyly of bryophytes with liverworts alone resolved as the earliest-branching land plant group. Here, we reconstruct the mitochondrial land plant phylogeny from a newly compiled data set. When among-lineage composition heterogeneity is accounted for in analyses of codon-degenerate nucleotide and amino acid data, the clade

36 Setophyta is recovered with high support, and hornworts are supported as the earliest-branching  
37 lineage of land plants. These new mitochondrial analyses demonstrate partial congruence with  
38 current hypotheses based on nuclear and chloroplast genome data, and provide further incentive  
39 for revision of how plants arose on land.

40

## 41 **Introduction**

42 The embryophytes, or land plants, share a green algal ancestor (McCourt, Delwiche & Karol  
43 2004) that colonized terrestrial environments between 515.1- 470.0 Ma (Morris et al. 2018) and  
44 comprise gametophyte-dominant lineages, collectively known as bryophytes, and a sporophyte-  
45 dominant lineage, the tracheophytes. Establishing the phylogenetic relationships between  
46 bryophytes (mosses, liverworts and hornworts) and tracheophytes (a monophyletic lineage that  
47 includes lycopods, ferns and seed plants) is therefore fundamental to understanding the evolution  
48 of plants on land. However, phylogenetic inferences of relationships among embryophytes drawn  
49 from molecular data of the nuclear (Finet et al. 2010; Wodniok et al. 2011; Wickett et al. 2014),  
50 chloroplast (Cox et al. 2014; Ruhfel et al. 2014; Zhong et al. 2013; Bell et al. 2020), and  
51 mitochondrial (Turmel, Otis & Lemieux 2013; Liu et al. 2014; Bell et al. 2020) genomes have  
52 long remained conflicting. These incongruences are likely due to molecular evolutionary  
53 processes that are especially apparent at deep timescales, such as multiple substitutions on the  
54 same site, that lead to loss of phylogenetic signal, and heterogeneity in substitution process  
55 patterns among sites and among lineages (Cox 2018). Phylogenetic patterns commonly observed  
56 among embryophytes included a sister-group relationship between hornworts and other  
57 embryophytes (Hedderon, Chapman & Rootes 1996; Malek et al. 1996; Nishiyama and Kato  
58 1999; Wickett et al. 2014), between liverworts and other embryophytes (Lewis, Mishler &  
59 Vilgalys 1997; Karol et al. 2001; Qiu et al. 2006; Gao, Su & Wang 2010; Karol et al. 2010;  
60 Clarke, Warnock & Donoghue 2011), or between embryophytes and a clade uniting mosses and  
61 liverworts (Karol et al. 2010). An alternative pattern shows an initial split between the bryophytes  
62 and the tracheophytes (Hori, Lim & Osawa 1985; Nishiyama et al. 2004; Goremykin and  
63 Hellwig 2005; Cox et al. 2014; Wickett et al. 2014; Puttick et al. 2018; Sousa et al. 2019;  
64 Leebens-Mack et al. 2019), implying the monophyly of both lineages. Nevertheless, the results  
65 are very much dependent on data and methodology, with authors typically presenting competing  
66 hypotheses. For instance, several recent phylogenomic analyses based on large nuclear data sets

67 and extensive taxon sampling (e.g. Wickett et al. 2014; Leebens-Mack et al. 2019) have been  
68 equivocal. These studies presented monophyletic-bryophyte phylogenies based on multi-species  
69 coalescent supertrees, but concatenated analyses of the same data resulted in trees in which the  
70 bryophytes were paraphyletic. Consequently, the authors were unable to provide arguments for  
71 which hypothesis was to be preferred. Indeed, the efficacy and suitability of using multi-species  
72 coalescent summary analyses versus concatenated data analyses for phylogenies with deep  
73 timescales is currently a topic of considerable debate (e.g. Tonini et al. 2015; Edwards et al.  
74 2016; Springer and Gatesy 2016). However, it should be noted that concatenated analyses of  
75 nuclear data do support a monophyletic bryophyte clade when modeling composition  
76 heterogeneity across the tree, although restricted analytical conditions, namely reduced taxon and  
77 site sampling, are currently necessary to decrease computational complexity when using tree-  
78 heterogeneous composition models. For instance, to use these models, Sousa et al (2019)  
79 analysed a reduced amino acid data set of 26 taxa and 100 genes, while Puttick et al. (2018)  
80 analysed Dayhoff-recoded data, that reduces the amino acid data to only six character states.  
81 Nevertheless, these tree-heterogeneous composition models are demonstrably better-fitting and  
82 are therefore likely more accurate and reliable than the analyses of larger data sets that used  
83 simpler and poorer-fitting models (Cox 2018).

84       Most analyses of land plant relationships have been based on chloroplast data and have  
85 typically shown the bryophytes to be paraphyletic (see Table 1 in Cox 2018). More recent  
86 phylogenetic analyses using models that account for saturation and composition tree-  
87 heterogeneity have, however, indicated that the bryophytes form a monophyletic group, and the  
88 authors provided arguments as to why these analyses using better-fitting models are to be  
89 preferred (Cox et al. 2014). In contrast, few land plant analyses of mitochondrial data have been  
90 presented, but all have indicated that the bryophytes form a paraphyletic group (i.e. Duff and  
91 Nickrent 1999; Groth-Maloney et al. 2004; Liu et al. 2014). The most recent and extensive  
92 phylogenetic analyses of plant mitochondrial genomes using tree-homogeneous composition  
93 models have shown that protein-coding nucleotide data place mosses as the sister-group to the  
94 remaining embryophytes, whereas amino acid data show a split between liverworts and the  
95 remaining embryophytes (Liu et al. 2014). However, this placement of liverworts as the sister-  
96 group to the remaining embryophytes contradicts recent nuclear and chloroplast phylogenies

97 which show high support for the clade Setaphyta, that groups liverworts with mosses (Cox et al.  
98 2014; Puttick et al. 2018; Sousa et al. 2019).

99 Our confidence in any evolutionary hypotheses regarding land plant relationships would  
100 increase greatly if phylogenetic inferences made from all three plant genomic compartments  
101 were not in conflict. In this study we investigate the mitochondrial phylogeny of land plants by  
102 applying better-fitting evolutionary models that account for composition tree-heterogeneity to a  
103 newly compiled data set of mitochondrial loci that includes sequences from three newly  
104 assembled genomes from the Coleochaetales and Zygnematales. We assemble a mitochondrial  
105 land plant data set of 26 taxa, which includes all major lineages of land plants and one of the  
106 putative most closely-related lineages to land plants, the Zygnematales. Assuming that both  
107 bryophytes and tracheophytes are likely monophyletic on the species tree (Sousa et al. 2019), the  
108 taxon sampling is deliberately restricted to include a proportional selection of bryophytes (11  
109 taxa) and tracheophytes (10) as symmetrical trees improve estimation (Huang and Knowles  
110 2009) and minimise long branch attraction (Philippe and Laurent 1998). Where possible, taxa  
111 were chosen to span what is currently considered the ancestral node of each bryophyte lineage  
112 (or the oldest ancestral node possible given the currently available data), thereby attempting to  
113 minimise the length of the sub-tending branch of each bryophyte clade and reduce long-  
114 branches. Most importantly, a smaller data set enables us to use better-fitting models that account  
115 for among-lineage and among-site composition heterogeneity that are computationally  
116 intractable for large data sets. This reduced sampling is in contrast to other studies which  
117 typically include many more taxa from highly derived lineages (especially angiosperms) whose  
118 inclusion, we maintain, has little impact on the resolution among major lineages (the question  
119 under consideration), but severely restricts the complexity of models that can be used and  
120 therefore the reliability of the inferences. Notably, a recent large-scale analysis of plant  
121 transcriptomes, despite the inclusion of 1155 taxa and 410 genes, was unable to resolve many of  
122 the long-standing contentious phylogenetic relationships, such as the relationships among the  
123 major lineages of land plants (Fig. 3 in Leebens-Mack et al. 2019). Indeed, rather than just  
124 including all available data injudiciously, and thereby restrict the complexity of models that can  
125 be applied for phylogenetic inference, it is important to consider which data should be included  
126 in a particular analysis: the choice of data should reflect carefully the question being addressed  
127 and its suitability for analysis by better-fitting models of molecular evolution.

128

129

## 130 **Materials & Methods**

131

### 132 *Sampling of mitochondrial genomes*

133 We sampled 21 taxa representing the major lineages of land plants, plus 5 green algae species as  
134 outgroup taxa. The taxa sampled for this study were: Coleochaetales (*Chaetosphaeridium*  
135 *globosum*, *Coleochaete scutata*), Zygnematales (*Closterium baillyanum*, *Gonatozygon*  
136 *brebissonii*, *Roya anglica*), liverworts (*Aneura pinguis*, *Marchantia polymorpha*, *Pleurozia*  
137 *purpurea*, *Treubia lacunosa*), mosses (*Atrichum angustatum*, *Bartramia pomiformis*,  
138 *Physcomitrella patens*, *Sphagnum palustre*, *Tetraphis pellucida*), hornworts (*Megaceros*  
139 *aenigmaticus*, *Phaeoceros laevis*), lycophytes (*Huperzia squarrosa*, *Isoetes engelmannii*),  
140 pteridophytes (*Ophioglossum californicum*, *Psilotum nudum*), and spermatophytes (*Brassica*  
141 *napus*, *Cycas taitungensis*, *Ginkgo biloba*, *Liriodendron tulipifera*, *Oryza sativa*, *Welwitschia*  
142 *mirabilis*).

143 Algal cultures for *Coleochaete scutata* (SAG 3.91) and *Gonatozygon brebissonii* (SAG  
144 292) were obtained from the Culture Collection of Algae (SAG) (Georg-August-Universität  
145 Göttingen, Germany), and the algal culture of *Roya anglica* (ACOI 799) was obtained from the  
146 Coimbra Collection of Algae (ACOI) (Universidade do Coimbra, Coimbra, Portugal). The  
147 mitochondrial genomes of the three taxa were sequenced and assembled *de-novo* using standard  
148 methods as described in (Civáň et al. 2014), and annotated with the aid of Mitofy (Alverson et al.  
149 2010) and NCBI BLAST analyses (Altschul et al. 1990). The remainder of the genomes were  
150 retrieved from NCBI GenBank (Bethesda, USA). The list of species samples, their classification,  
151 and the source and accession numbers of the sequences used are shown in Table 1.

152

### 153 *Alignment and model testing*

154 The sequences of each of 43 mitochondrial protein-coding genes were aligned using the program  
155 MAFFT (vers. 6.8; Katoh and Toh 2008). Nucleotide alignments were manually edited in  
156 Geneious (vers. 9; <http://www.geneious.com>) to remove out-of-frame indels, misaligned  
157 portions, premature stop codons, positions with less than 50% taxon occupancy, and ambiguities.  
158 Genes that were missing with the algal outgroup taxa (Coleochaetales and Zygnematales) or

159 were under 200 bp in length were discarded. The final data set consisted of 36 genes for 26 taxa,  
160 with a missing gene occupancy of 9.5%. Amino acid alignments were generated by translation  
161 from each of the 36 nucleotide matrices using SeaView (vers. 4.5.4; Gouy, Guindon & Gascuel  
162 2009). The best-fitting substitution models for the 36 amino acid alignments were inferred in  
163 PartitionFinder (Lanfear et al. 2012) using the BIC selection criterion. The stmtREV (Liu et al.  
164 2014) with a gamma-distribution of among-site rates (+G) model was the best-fitting model for  
165 all genes but one, for which the chosen model was JTT+G (Jones, Taylor & Thornton 1992).

166

### 167 *Gene tree estimation and monophyly test*

168

169 Gene trees were estimated from individual nucleotide matrices, using the general time-reversible  
170 model (Rodriguez et al. 1990) with a gamma rate distribution and estimated base frequencies  
171 (GTR+G+F<sub>est</sub>), and from amino acid matrices, using the best-fitting models inferred  
172 inPartitionFinder (stmtREV+G+F<sub>est</sub>, JTT+G+F<sub>est</sub>). Bayesian MCMC analyses were performed  
173 with P4 (Foster 2004) using tree-homogeneous (henceforth referred to as CV1, i.e. one  
174 composition vector) and tree-heterogeneous (NDCH) composition models. Each analysis had  
175 two independent runs which were assessed for convergence by calculation of the marginal  
176 likelihood (chains were considered to have converged if they differed by <10 units) and the  
177 average standard-deviation of split support between trees sampled from the posterior  
178 distributions (chains were considered to have converged if <0.01). Posterior predictive  
179 simulations of the  $X^2$  test statistic of composition homogeneity was used to assess composition  
180 fit (Foster 2004). For each gene, 50% majority-rule consensus trees were generated from the  
181 best-fitting analyses of the nucleotide and amino acid data.

182 Gene tree topologies inferred from each of the 36 amino acid alignments were tested  
183 using “gene genealogy interrogation” (GGI; Arcila et al. 2017) to ascertain whether the non-  
184 monophyly of the five major lineages under scrutiny (hornworts, liverworts, mosses,  
185 tracheophytes, and the outgroups) was statistically supported by the data. We were to consider  
186 any gene that supported the non-monophyly of one of these clades as aberrant and not suitable  
187 for inclusion in the combined analyses, as the monophyly of hornworts, liverworts, mosses,  
188 tracheophytes and embryophytes has been consistently recovered in molecular phylogenies (e.g.  
189 Qiu *et al.* 2006; Liu *et al.* 2014). Optimal trees for each gene were compared to each of fifteen

190 constraint trees representing all possible topologically resolved combinations of the five  
191 monophyletic groups, using a nonparametric bootstrapping test. The results were assessed for  
192 statistical significance with the Approximately Unbiased (AU) test (Shimodaira 2002) in  
193 CONSEL (vers. 0.1k; Shimodaira and Hasegawa 2001). Optimal trees were estimated in  
194 RAxML (MPI-compiled vers. 8.2.8; Stamatakis 2014) using the model stntREV+G+F<sub>est</sub> and  
195 starting from 20 random trees. Constraint trees were written in Newick format with internal  
196 branches within each of the five major clades collapsed to a polytomy. Each constraint tree was  
197 optimized in RAxML under the stntREV+G+F<sub>est</sub> model. Constraint topologies were considered  
198 statistically supported by the data if the p-value of the AU test was equal or greater than 0.05,  
199 meaning that the monophyly of each of the five lineages could not be rejected. In every gene, at  
200 least one of the constraint topologies was supported by the data, meaning that the monophyly of  
201 each clade could not be rejected, thus all 36 genes were included in downstream analyses.

202

### 203 *Analyses of concatenated nucleotide data*

204 A nucleotide alignment with 24,864 characters was obtained from the concatenation of the 36  
205 individual genes. A second concatenated nucleotide matrix was constructed by codon-degenerate  
206 recoding of the data where ambiguity codes are used to negate synonymous substitutions  
207 (Criscuolo and Gribaldo 2010; Cox et al. 2014). Bayesian MCMC analyses were performed on  
208 the concatenated and codon-degenerate nucleotide matrices using a tree-homogeneous  
209 composition model (CV1; 2 replicates) and the tree-heterogeneous composition (NDCH2; 4  
210 replicates) model, as implemented on P4. In contrast to the original NDCH model (Foster 2004)  
211 that allows an *a priori* defined number of compositions to evolve on the tree, the NDCH2 model  
212 estimates a separate composition for each node of the tree, constrained by a sampled Dirichlet  
213 prior on how much the composition vectors may differ from the empirical composition. Model  
214 fit to composition heterogeneity was inferred during the Bayesian MCMC with posterior  
215 predictive simulations of the  $X^2$  statistic of composition homogeneity, where p-values equal or  
216 greater than 0.05 indicate acceptance of the model. The GTR+G+F<sub>est</sub> model of substitution was  
217 used for for all MCMC of nucleotide and degenerate nucleotide data. Marginal likelihoods were  
218 estimated in P4 according to the Eqn 16 method of Newton and Raftery (1994).

219

### 220 *Analyses of concatenated amino acid data*

221 An amino acid alignment with 8,288 characters was obtained by concatenation of the amino acid  
222 translations of the 36 genes. Bayesian MCMC analysis was performed on the concatenated  
223 amino acid data using both tree-homogeneous composition (stmtREV+G+F<sub>CV1</sub>; 2 replicates) and  
224 tree-heterogeneous composition (stmtREV+G+F<sub>NDCH2</sub>; 4 replicates) models, with the fit of the  
225 composition evaluated by posterior predictive simulations as described for the nucleotide data. In  
226 addition, a Bayesian MCMC analysis was also performed using PhyloBayes (MPI-compiled  
227 vers. 1.6; Lartillot, Lepage & Blanquart 2009) under the model stmtREV+G+F<sub>CAT</sub>.

228 Alignments of individual genes, the concatenated data, and the resulting tree files of each  
229 analysis are available on Zenodo (doi: 10.5281/zenodo.3554149). All ML analyses of the  
230 concatenated nucleotide and amino acid data sets were consistent with the homogeneous  
231 Bayesian MCMC analyses and are not reported here, but the resulting tree files are also available  
232 on Zenodo.

233

## 234 **Results**

### 235 *Nucleotide and codon-degenerate data*

236 All individual genes were best-fit by a tree-heterogeneous composition model with two  
237 composition vectors on the tree (CV2; Table S1). Majority-rule consensus trees resulting from  
238 the best-fitting Bayesian MCMC analyses of individual genes had low resolution in general, but  
239 liverworts were supported (> 95% posterior probability (PP)) as the earliest-branching lineage in  
240 two genes (*nad3* and *nad5*), whereas the mosses were supported as the earliest-branching lineage  
241 in one gene (*ccmC*). All other resolutions of the bryophyte lineages relative to the tracheophyte  
242 clade were not statistically supported, and the Setaphyta clade was not resolved in any gene tree.

243 Bayesian MCMC analysis of the concatenated nucleotide data set, assuming a  
244 homogeneous composition (CV1), resulted in a tree with mosses as the sister-group to the  
245 remaining land plants (PP= 1.0; Figure 1a; Figure S1), and hornworts as sister-group to the  
246 tracheophytes (PP= 1.0). In contrast, the analysis of the degenerate data set under a  
247 homogeneous base composition (Figure 1c; Figure S2) returned a tree with liverworts the  
248 earliest-branching lineage of embryophytes (PP= 1.0) and hornworts the sister-group to  
249 tracheophytes (PP= 0.93). However, the homogeneous model was rejected for both data sets by  
250 the posterior predictive simulation of the  $X^2$  statistics of homogeneity, with a tail-area probability  
251 of 0.0, thereby indicating that the data were not composition homogeneous. The tree-

252 heterogeneous composition analysis (NDCH2) of the concatenated nucleotide data also resulted  
253 in mosses supported as the earliest-diverging land plant lineage (PP= 0.98; Figure 1b; Figure  
254 S3), but placed liverworts as the sister-group to tracheophytes (PP= 0.94). The NDCH2 model  
255 was a good fit to the data according to the posterior predictive simulation ( $X^2$  p= 0.99). When  
256 analysing the codon-degenerate data, the NDCH2 model recovered hornworts as the sister-group  
257 to the remaining land plants with full branch support (PP= 1.0; Figure 1d; Figure S4), and  
258 mosses fully supported (PP= 1.0) as the sister-group to liverworts (i.e. the clade Setaphyta). The  
259 NDCH2 model was not a good statistical fit to the data for the best scoring MCMC run,  
260 according to the  $X^2$  posterior predictive test ( $X^2$  p= 0.038; Figure S4).

261

#### 262 *Amino acid data*

263 Individual mitochondrial protein alignments were best-fit by both homogeneous and  
264 heterogeneous composition models, with some being best-fit by a model with up to four  
265 compositions (CV4), indicating that they are highly heterogeneous in composition among  
266 lineages (Table S1). Majority-rule consensus trees of best-fitting Bayesian MCMC analyses of  
267 individual proteins were poorly supported regarding relationships among bryophyte lineages.  
268 Indeed, only one tree (*ccmC*) showed any statistically supported resolution and placed the  
269 mosses as the earliest-branching lineage of embryophytes. Although not statistically supported,  
270 one amino-acid tree showed bryophytes as a monophyletic group (*rps7*), and the clade Setaphyta  
271 was present in three others (*atp4*, *rpl2*, and *sdh4*).

272 When the concatenated amino acid data were analysed with a tree-homogeneous  
273 composition model (CV1), the resulting tree recovered liverworts as the sister-group to the  
274 remaining embryophytes without statistically significant support (PP= 0.82), and hornworts as  
275 the sister-group to tracheophytes, also without support (PP= 0.82; Figure 1e; Figure S5). The  
276 homogeneous composition model did not fit the data ( $X^2$  p= 0.0). The Phylobayes  
277 *stmtREV+G+F<sub>CAT</sub>* analysis (stationary, data-heterogeneous composition model) of the  
278 concatenated amino acid data resulted in an unsupported placement of liverworts as the sister-  
279 group to the remaining embryophytes (PP= 0.89; Figure S6). A posterior predictive composition  
280 homogeneity test using Phylobayes (*readpb\_mpi* parameter *-comp*) showed that the data rejected  
281 the model and that the data were therefore composition tree-heterogeneous (p= 0.0). When the  
282 tree-heterogeneous composition NDCH2 model was used to model the concatenated protein data,

283 the separate analyses did not converge on the same tree topology, although the NDCH2 model  
284 was a good fit ( $X^2$   $p=0.1022$ ). The tree obtained from the analyses with the best marginal  
285 likelihood ( $-\ln L_h$  142829.1129) supported hornworts as the earliest-branching lineage (PP= 1.0),  
286 with the liverworts as the sister-group to mosses (PP=1.0; Figs. 1f, 2, S7).

287

## 288 Discussion

289

290 *Gene tree discordance in mitochondrial data is likely due to mis-modeling and insufficient*  
291 *phylogenetic signal*

292 Alternative hypothesis testing using nonparametric and parametric bootstrapping has been  
293 applied before to the mitochondrial land plant phylogeny to test the fit of the data (Liu et al.  
294 2014). Here we chose a different approach, and used the optimized likelihood of constraint trees  
295 to identify genes that did not support the monophyly of the major embryophyte lineages  
296 (hornworts, liverworts, mosses, and tracheophytes) and of the outgroup. The optimal trees of the  
297 36 mitochondrial genes, inferred under maximum-likelihood, show varied topologies, among  
298 which none is predominant. Because the four major land plant lineages are known to be  
299 monophyletic (as shown by many studies, e.g. Wickett et al. 2014) our concern was to identify  
300 gene trees that showed non-monophyly of one of these groups. The strategy we adopted allowed  
301 us to discern whether such topologies truly reflect underlying data or whether they are one  
302 among different topologies supported by the data. The AU test indicated, in all genes, that the  
303 monophyly of each land plant lineage was not statistically contradicted. This result suggests that  
304 the observed phylogenetic conflict among mitochondrial gene trees is unlikely to be explained by  
305 biological processes, such as horizontal gene transfer or duplication-loss, affecting specific  
306 lineages within each of the four major groups, and that any observed paraphyly of major groups  
307 on gene trees is probably the result of inadequate data modeling or paucity of phylogenetic  
308 signal.

309

310 *Synonymous substitutions are responsible for the placement of mosses as the earliest-branching*  
311 *lineage of embryophytes*

312 The tree inferred from the concatenated nucleotide data set of 36 mitochondrial genes shows  
313 mosses as the sister-group to the remaining land plants, as previous analyses of mitochondrial

314 nucleotide data have shown (Liu et al. 2014). However, the mosses are replaced by the liverworts  
315 in the same position when analysing codon-degenerate recoded data. Codon degenerate recoding  
316 is used to eliminate synonymous substitutions, which are unconstrained by selection at the  
317 protein level and therefore can be subject to high rates of substitution, and ultimately saturation  
318 and loss of phylogenetic signal. Indeed, as the exclusion of synonymous substitutions is  
319 sufficient to eliminate phylogenetic signal that supports mosses as the sister-group to the  
320 remaining land plants, these results illustrate that despite being the slowest evolving genomic  
321 compartment in plants, phylogenetic inferences from highly divergent mitochondrial genomes  
322 are also affected by substitutional saturation due to the effect of high substitution rates.  
323 Moreover, this observation implies that caution should be taken when invoking biological  
324 explanations (e.g. hybridisation, incomplete lineage sorting) to explain incongruence among  
325 phylogenies when inadequate modeling of the substitution process may represent a simpler  
326 explanation.

327

328 *Codon degenerate nucleotide data and protein data support Setaphyta under tree-heterogeneous*  
329 *models of substitution*

330 With the nucleotide data, both the tree-homogeneous and NDCH2 tree-heterogeneous models  
331 support mosses as the earliest-diverging group in the embryophytes. The likely incorrect  
332 placement of mosses as the earliest-diverging group that is recovered with the best-fitting tree-  
333 heterogeneous NDCH2 model suggests that homoplasy driven by high nucleotide substitution  
334 rates (saturation) may overwhelm the ability of the model to correct for composition bias, hence  
335 the need to use codon-degenerate recoded data in combination with tree-heterogeneous models.  
336 Indeed, when codon-degenerate recoded data are used, contrasting supported relationships are  
337 obtained under tree-homogeneous and tree-heterogeneous composition models. Whereas using a  
338 homogeneous model for the analysis of the codon-degenerate data shows liverworts well  
339 supported as the sister-group to other embryophytes, the tree-heterogeneous analysis (NDCH2)  
340 model places liverworts as the sister-group to the mosses (clade Setaphyta), with maximum  
341 support, and hornworts as the sister-group to all other embryophytes, also with maximum branch  
342 support. These results demonstrate that the phylogenetic signal contained in non-synonymous  
343 sites is also subject to composition biases and that tree-heterogeneous composition models are  
344 required to model the data effectively. Contrasting results were also obtained when the amino

345 acid data were analysed with tree-homogeneous and tree-heterogeneous models. The tree  
346 inferred under the poorly-fitting ( $P=0.0$ ) homogeneous model (CV1) resolves liverworts as the  
347 sister-group to the remaining land plants ( $PP=0.82$ ). By contrast, the Bayesian MCMC run with  
348 the highest marginal likelihood under the NDCH2 (fitting) model shows strong support for the  
349 Setaphyta clade ( $PP= 1.0$  – mosses plus liverworts) with the hornworts as the earliest-branching  
350 lineage of embryophytes ( $PP= 1.0$ ). Liu et al. (2014) observed topological congruence between  
351 mitochondrial nucleotide and protein data that placed liverworts as the sister-group to all other  
352 embryophytes, but this placement of liverworts received low branch support in different  
353 analyses, and thus no firm conclusions regarding these cladogenic events were put forward.  
354 Importantly, in that study no tree-heterogeneous analyses of the codon-degenerate data were  
355 performed, nor was the protein data analysed with more than two composition vectors on the  
356 tree. In contrast, our analyses of the codon-degenerate nucleotide data and amino acid data using  
357 a better-fitting tree-heterogeneous model resulted in well supported, congruent topologies,  
358 strengthening the argument in favour of the analyses presented here, that show support for the  
359 clade Setaphyta.

360

361 *The land plant mitochondrial phylogeny is partially congruent with nuclear and chloroplast*  
362 *phylogenies*

363 In contrast to previous analyses of the land plant mitochondrial phylogeny, we show that both  
364 nucleotide and amino acid data carry signal that joins mosses and liverworts as sister lineages  
365 (clade Setaphyta). This phylogenetic signal is typically obscured due to substitution saturation in  
366 the nucleotide data and among-lineage composition bias in both the nucleotide and amino acid  
367 data. In the nucleotide data, phylogenetic signal supporting mosses as the sister-group to the  
368 remaining land plants is eliminated when codon-degenerate recoded data is analysed, and instead  
369 the liverworts are found as the sister-group to all the remaining embryophytes under tree-  
370 homogeneous composition models. However, it is only when a combination of codon-degenerate  
371 recoding and a better-fitting tree-heterogeneous composition model is used that the mosses and  
372 liverworts appear resolved as sister taxa, therefore suggesting that both substitutional saturation  
373 and among-lineage composition heterogeneity are important evolutionary processes to be  
374 modeled in the nucleotide data. Similarly, the unsupported placement of liverworts as the  
375 earliest-branching lineage is obtained using tree-homogeneous composition models with the

376 amino acid data, but better-fitting tree-heterogeneous composition models again support the  
377 mosses plus liverwort clade.

378 Support for the moss-liverwort sister-group relationship has been found in trees  
379 previously inferred from nuclear and chloroplast protein-coding data (e.g. Nishiyama et al. 2004;  
380 Cox et al. 2014; Puttick et al. 2018; Sousa et al. 2019). The clade can be resolved by  
381 mitochondrial data with our analyses, and therefore avoids the necessity of calling upon  
382 biological explanations, such as hybridisation, to account for incongruence among the  
383 phylogenies of the three plant genomes regarding the placement of mosses and liverworts.  
384 However, if the placement of the hornworts as the earliest-branching lineage of embryophytes  
385 does indeed reflect the true mitochondrial topology, then it is in conflict with the nuclear and  
386 chloroplast data which suggest the bryophytes are likely monophyletic. A biological process  
387 involving a rapid divergence of the hornworts from other bryophytes, after the tracheophyte-  
388 bryophyte split, and the retention of a copy of the mitochondrion that was lost in all other  
389 embryophyte lineages, could be invoked to explain the observed phylogenetic conflict. However,  
390 the incongruence of the mitochondrial data could, of course, still be a result of mis-modeling or  
391 lack of phylogenetic signal. It is likely that further sampling of mitochondrial genomes from  
392 hornworts and other bryophyte lineages may aid resolution of the phylogeny, but such analyses  
393 would only be informative if they were in combination with the heterogeneous composition  
394 models that have been shown here to be necessary to correctly model the underlying processes of  
395 mitochondrial evolution.

396

397

## 398 **Conclusions**

399

400 The main contribution of this study is the demonstration that liverworts are not the sister-group  
401 to embryophytes in the land plant mitochondrial phylogeny, unlike earlier analyses of  
402 mitochondrial genomes suggested (Liu et al. 2014). Instead, strong support is found for the clade  
403 Setaphyta, corroborating support for this clade found in nuclear and plastid genomes, and  
404 showing that the mitochondrial phylogeny of land plants is not strongly incongruent with the  
405 nuclear and plastid phylogenies. Although the best-scoring tree found by analyses of amino acid  
406 data places hornworts as sister-group to embryophytes, the monophyly of bryophytes, which is

407 supported by evidence from nuclear and plastid genomes, cannot be strongly rejected.  
408 Importantly, this study also shows that modeling of composition tree-heterogeneity in amino acid  
409 data must not be disregarded, even in slower-evolving genomic regions such as plant  
410 mitochondria.

411

412

413

## 414 **References**

415

416 Alverson AJ, Wei XX, Rice DW, Stern DB, Barry K, Palmer JD. 2010. Insights into the  
417 evolution of mitochondrial genome size from complete sequences of *Citrullus lanatus* and  
418 *Cucurbita pepo* (Cucurbitaceae). *Molecular Biology and Evolution* 27: 1436–1448.

419 Altschul SF, Gish W, Miller W, Myers EW, Lipman DJ. 1990. Basic local alignment search tool.  
420 *Journal of Molecular Biology* 215: 403–410.

421 Arcila D, Ortí G, Vari R, Armbruster JW, Stiassny ML, Ko KD, Sabaj MH, Lundberg J, Revell  
422 LJ, Betancur-R R. 2017. Genome-wide interrogation advances resolution of recalcitrant  
423 groups in the tree of life. *Nature Ecology & Evolution* 1: 0020.

424

425 Bell, D., Lin, Q., Gerelle, W. K., Joya, S., Chang, Y., Taylor, Z. N., Rothfels, C.J., Larsson, A.,  
426 Villarreal, J.C., Li, F.-W., Pokorny, L., Szövényi, P., Crandall-Stotler, B., DeGironimo, L.,  
427 Floyd, S.K., Beerling, D.J., Deyholos, M.K., von Konrat, M., Ellis, S., Shaw, A.J., Chen,  
428 T., Wong, G.K.-S., Stevenson, D.W., Palmer, J.D., Graham, S.W. (2020). Organellomic  
429 data sets confirm a cryptic consensus on (unrooted) land-plant relationships and provide  
430 new insights into bryophyte molecular evolution. *American Journal of Botany* 107: 91-115.

431 Civaň P, Foster PG, Embley MT, Seneca A, Cox CJ. 2014. Analyses of charophyte chloroplast  
432 genomes help characterize the ancestral chloroplast genome of land plants. *Genome  
433 Biology and Evolution* 6: 897–911.

434 Clarke JT, Warnock RCM, Donoghue PCJ. 2011. Establishing a time-scale for plant evolution.  
435 *New Phytologist* 192: 266–301.

- 436 Cox CJ, Li B, Foster PG, Embley TM, Civián P. 2014. Conflicting phylogenies for early land  
437 plants are caused by composition biases among synonymous substitutions. *Systematic*  
438 *Biology* 63: 272–279.
- 439 Cox CJ. 2018. Land plant molecular phylogenetics: a review with comments on evaluating  
440 incongruence among phylogenies. *Critical Reviews in Plant Sciences* 37: 113–127.
- 441 Criscuolo A, Gribaldo S. 2010. BMGE (Block Mapping and Gathering with Entropy): a new  
442 software for selection of phylogenetic informative regions from multiple sequence  
443 alignments. *BMC Evolutionary Biology* 10: 210.
- 444 Duff RJ, Nickrent DL. 1999. Phylogenetic relationships of land plants using mitochondrial small  
445 subunit rDNA sequences. *American Journal of Botany* 86: 372-386.
- 446 Edwards SV, Xi Z, Janke A, Faircloth BC, McCormack JE, Glenn TC, Zhong B, Wu S, Lemmon  
447 EM, Lemmon AR, Leaché AD. 2016. Implementing and testing the multispecies  
448 coalescent model: a valuable paradigm for phylogenomics. *Molecular Phylogenetics and*  
449 *Evolution* 94: 447–462.
- 450 Finet C, Timme RE, Delwiche CF, Marlétaz F. 2010. Multigene phylogeny of the green lineage  
451 reveals the origin and diversification of land plants. *Current Biology* 20: 2217–2222.
- 452 Foster PG. 2004. Modeling compositional heterogeneity. *Systematic Biology* 53: 485–495.
- 453 Gao L, Su YJ, Wang T. 2010. Plastid genome sequencing, comparative genomics, and  
454 phylogenomics: Current status and prospects. *Journal of Systematics and Evolution* 48:  
455 77–93.
- 456 Goremykin VV, Hellwig FH. 2005. Evidence for the most basal split in land plants dividing  
457 bryophyte and tracheophyte lineages. *Plant Systematics and Evolution* 254: 93-103.
- 458 Gouy M, Guindon S, Gascuel O. 2009. SeaView version 4: a multiplatform graphical user  
459 interface for sequence alignment and phylogenetic tree building. *Molecular Biology and*  
460 *Evolution* 27: 221–224.
- 461 Groth-Malonek M, Pruchner D, Grewe F, Knoop V. 2004. Ancestors of trans-splicing  
462 mitochondrial introns support serial sister group relationships of hornworts and mosses  
463 with vascular plants. *Molecular Biology and Evolution* 22: 117–125.
- 464 Hedderson TA, Chapman RL, Rootes, WL. 1996. Phylogenetic relationships of bryophytes  
465 inferred from nuclear-encoded rRNA gene sequences. *Plant Systematics and Evolution*  
466 200: 213-224.

- 467 Hori H, Lim B-L, Osawa S. 1985. Evolution of green plants as deduced from 5S rRNA  
468 sequences. *Proceedings of the National Academy of Sciences U. S. A.* 82: 820–823.
- 469 Huang H, Knowles LL. 2009. What is the danger of the anomaly zone for empirical  
470 phylogenetics? *Systematic Biology* 58: 527–536.
- 471 Jones DT, Taylor WR, Thornton JM. 1992. The rapid generation of mutation data matrices from  
472 protein sequences. *Bioinformatics* 8: 275–282.
- 473 Karol KG, McCourt RM, Cimino MT, Delwiche CF. 2001. The closest living relatives of land  
474 plants. *Science* 294: 2351–2353.
- 475 Karol KG, Karol KG, Arumuganathan K, Boore JL, Duffy AM, Everett KD, Hall JD, Hansen  
476 SK, Kuehl JV, Mandoli DF, Mishler BD, Olmstead RG. 2010. Complete plastome  
477 sequences of *Equisetum arvense* and *Isoetes flaccida*: implications for phylogeny and  
478 plastid genome evolution of early land plant lineages. *BMC Evolutionary Biology* 10: 321.
- 479 Katoh K, Toh H. 2008. Recent developments in the MAFFT multiple sequence alignment  
480 program. *Brief. Bioinformatics* 9: 286–298.
- 481 Lanfear R, Calcott B, Ho SY, Guindon S. 2012. PartitionFinder: combined selection of  
482 partitioning schemes and substitution models for phylogenetic analyses. *Molecular Biology  
483 and Evolution* 29: 1695–1701.
- 484 Lartillot N, Lepage T, Blanquart S. 2009. PhyloBayes 3: a Bayesian software package for  
485 phylogenetic reconstruction and molecular dating. *Bioinformatics* 25: 2286–2288.
- 486 Leebens-Mack J, Barker M, Carpenter E, Deyholos M, Gitzendanner M, Graham S, Grosse I, Li  
487 Z, Melkonian M, Mirarab S, Porsch M, Quint M, Rensing S, Soltis D, Soltis P, Stevenson  
488 D, Ullrich K, Wickett N, DeGironimo L, Edger P, Jordon-Thaden I, Joya S, Liu T,  
489 Melkonian B, Miles N, Pokorny L, Quigley C, Thomas P, Villarreal J, Augustin M, Barrett  
490 M, Baucom R, Beerling D, Benstein R, Biffin E, Brockington S, Burge D, Burris J, Burris  
491 K, Burtet-Sarramegna V, Caicedo A, Cannon S, Cebi Z, Chang Y, Chater C, Cheeseman  
492 J, Chen T, Clarke N, Clayton H, Covshoff S, Crandall-Stotler B, Cross H, DePamphilis C,  
493 Der J, Determann R, Dickson R, Di Stilio V, Ellis S, Fast E, Feja N, Field K, Filatov D,  
494 Finnegan P, Floyd S, Fogliani B, Garcia N, Gateble G, Godden G, Goh Q.-Y, Greiner S,  
495 Harkess A, Heaney J, Helliwell K, Heyduk K, Hibberd J, Hodel R, Hollingsworth P,  
496 Johnson M, Jost R, Joyce B, Kapralov M, Kazamia E, Kellogg E, Koch M, Von Konrat M,  
497 Konyves K, Kutchan T, Lam V, Larsson A, Leitch A, Lentz R, Li F.-W, Lowe A, Ludwig

- 498 M, Manos P, Mavrodiev E, McCormick M, McKain M, McLellan T, McNeal J, Miller R,  
499 Nelson M, Peng Y, Ralph P, Real D, Riggins C, Ruhsam M, Sage R, Sakai A, Scascitella  
500 M, Schilling E, Schlosser E.-M, Sederoff H, Servick S, Sessa E, Shaw A, Shaw S, Sigel E,  
501 Skema C, Smith A, Smithson A, Stewart C, Stinchcombe J, Szovenyi P, Tate J, Tiebel H,  
502 Trapnell D, Villegente M, Wang C.-N, Weller S, Wenzel M, Weststrand S, Westwood J,  
503 Whigham D, Wu S, Wulff A, Yang Y, Zhu D, Zhuang C, Zuidof J, Chase M, Pires J,  
504 Rothfels C, Yu J, Chen C, Chen L, Cheng S, Li J, Li R, Li X, Lu H, Ou Y, Sun X, Tan X,  
505 Tang J, Tian Z, Wang F, Wang J, Wei X, Xu X, Yan Z, Yang F, Zhong X, Zhou F, Zhu Y,  
506 Zhang Y, Ayyampalayam S, Barkman T, Nguyen N.-P, Matasci N, Nelson D, Sayyari E,  
507 Wafula E, Walls R, Warnow T, An H, Arrigo N, Baniaga A, Galuska S, Jorgensen S,  
508 Kidder T, Kong H, Lu-Irving P, Marx H, Qi X, Reardon C, Sutherland B, Tiley G, Welles  
509 S, Yu R, Zhan S, Gramzow L, Theissen G, Wong G. K.-S. 2019. One thousand plant  
510 transcriptomes and the phylogenomics of green plants. *Nature* 574: 679–685.
- 511 Lewis LA, Mishler BD, Vilgalys R. 1997. Phylogenetic relationships of the liverworts  
512 (Hepaticae), a basal embryophyte lineage, inferred from nucleotide sequence data of the  
513 chloroplast gene *rbcL*. *Molecular Phylogenetics and Evolution* 7: 377–393
- 514 Liu Y, Cox CJ, Wang W, Goffinet B. 2014. Mitochondrial phylogenomics of early land plants:  
515 Mitigating the effects of saturation, compositional heterogeneity, and codon-usage bias.  
516 *Systematic Biology* 63: 862–878.
- 517 Malek O, Lüttig K, Hiesel R, Brennicke A, Knoop V. 1996. RNA editing in bryophytes and a  
518 molecular phylogeny of land plants. *The EMBO Journal* 15: 1403–1411.
- 519 McCourt RM, Delwiche CF, Karol KG. 2004. Charophyte algae and land plant origins. *Trends in*  
520 *Ecology & Evolution* 19: 661–666.
- 521 Morris JL, Morris JL, Puttick MN, Clark JW, Edwards D, Kenrick P, Pressel S, Wellman CH,  
522 Yang Z, Schneider H, Donoghue PC. 2018. The timescale of early land plant evolution.  
523 *Proceedings of the National Academy of Sciences U. S. A.* 115: E2274–E2283.
- 524 Newton MA, Raftery AE. 1994. Approximate Bayesian inference with the weighted likelihood  
525 bootstrap. *Journal of the Royal Statistical Society B* 56: 3–48.
- 526 Nishiyama T, Nishiyama T, Wolf PG, Kugita M, Sinclair RB, Sugita M, Sugiura C, Wakasugi T,  
527 Yamada K, Yoshinaga K, Yamaguchi K, Ueda K. 2004. Chloroplast phylogeny indicates  
528 that bryophytes are monophyletic. *Molecular Biology and Evolution* 21: 1813–1819.

- 529 Nishiyama T, Kato M. 1999. Molecular phylogenetic analysis among bryophytes and  
530 tracheophytes based on combined data of plasmid coded genes and the 18S rRNA gene.  
531 *Molecular Biology and Evolution* 16: 1027–1036.
- 532 Philippe H, Laurent J. 1998. How good are deep phylogenetic trees? *Current Opinion in*  
533 *Genetics and Development* 8: 616–623.
- 534 Puttick MN, Morris JL, Williams TA, Cox CJ, Edwards D, Kenrick P, Pressel S, Wellman CH,  
535 Schneider H, Pisani D, Donoghue PC. 2018. The interrelationships of land plants and the  
536 nature of the ancestral embryophyte. *Current Biology* 28: 733–745.
- 537 Qiu Y-L, Li L, Wang B, Chen Z, Knoop V, Groth-Malonek M, Dombrowska O, Lee J, Kent L,  
538 Rest J, Estabrook GF. 2006. The deepest divergences in land plants inferred from  
539 phylogenomic evidence. *Proceedings of the National Academy of Sciences U. S. A.* 103:  
540 15511–15516.
- 541 Rodriguez F, Oliver JL, Marin A, Medina JR. 1990. The general stochastic model of nucleotide  
542 substitution. *Journal of Theoretical Biology* 142: 485-501.
- 543 Ruhfel BR, Gitzendanner MA, Soltis PS, Soltis DE, Burleigh JG. 2014. From algae to  
544 angiosperms--inferring the phylogeny of green plants (Viridiplantae) from 360 plastid  
545 genomes. *BMC Evolutionary Biology* 14: 23.
- 546 Shimodaira H. 2002. An approximately unbiased test of phylogenetic tree selection. *Systematic*  
547 *Biology* 51: 492–508.
- 548 Shimodaira H, Hasegawa M. 2001. CONSEL: for assessing the confidence of phylogenetic tree  
549 selection. *Bioinformatics* 17:1246–1247.
- 550 Sousa F, Foster PG, Donoghue PC, Schneider H, Cox CJ. 2019. Nuclear protein phylogenies  
551 support the monophyly of the three bryophyte groups (Bryophyta Schimp.). *New*  
552 *Phytologist* 222: 565–575.
- 553 Springer MS, Gatesy J. 2016. The gene tree delusion. *Molecular Phylogenetics and Evolution*  
554 94, 1-33.
- 555 Stamatakis A. 2014. RAxML version 8: a tool for phylogenetic analysis and post-analysis of  
556 large phylogenies. *Bioinformatics* 30: 1312-1313.
- 557 Tonini J, Moore A, Stern D, Shcheglovitova M, Ortí G. 2015. Concatenation and species tree  
558 methods exhibit statistically indistinguishable accuracy under a range of simulated  
559 conditions. *PLoS currents*, 7.

- 560 Turmel M, Otis C, Lemieux C. 2013. Tracing the evolution of streptophyte algae and their  
561 mitochondrial genome. *Genome Biology and Evolution* 5: 1817–1835.
- 562 Wickett NJ, Mirarab S, Nguyen N, Warnow T, Carpenter C, Matasci N, Ayyampalayam S,  
563 Barker MS, Burleigh JG, Gitzendanner MA, Ruhfel BR, Wafula E, Der JP, Graham SW,  
564 Mathews S, Melkonian M, Soltis DE, Soltis PS, Miles NW, Rothfels C-J, Pokorny L,  
565 Shaw AJ, DeGironimo L, Stevenson DW, Surek B, Villarreal JC, Roure B, Philippe H,  
566 dePamphilis CW, Chen T, Deyholos MK, Baucom RS, Kutchan TM, Augustin MM, Wang  
567 J, Zhang Y, Tian Z, Yan Z, Wu X, Sun X, Wong GK-S, Leebens-Mack J. 2014.  
568 Phylotranscriptomic analysis of the origin and early diversification of land plants.  
569 *Proceedings of the National Academy of Sciences U. S. A.* 111: E4859–E4868.
- 570 Wodniok S, Brinkmann H, Glöckner G, Heidel AJ, Philippe H, Melkonian M, Becker B. 2011.  
571 Origin of land plants: do conjugating green algae hold the key? *BMC Evolutionary Biology*  
572 11: 104.
- 573 Zhong B, Xi Z, Goremykin VV, Fong R, Mclenachan PA, Novis PM, Davis CC, Penny D. 2013.  
574 Streptophyte algae and the origin of land plants revisited using heterogeneous models with  
575 three new algal chloroplast genomes. *Molecular Biology and Evolution* 31: 177-183.  
576

**Table 1** (on next page)

Accession table of the 26 samples used in this study.

For each species, the corresponding taxonomic group and NCBI GenBank accession numbers are shown. Accessions marked with an asterisk (\*) correspond to newly assembled genomes.

1

species	taxonomic group	Accession
<i>Closterium baillyanum</i>	Zygnematales	NC_022860
<i>Gonatozygon brebissonii</i>	Zygnematales	MK720950 *
<i>Roya anglica</i>	Zygnematales	MK720948 *
<i>Chaetosphaeridium globosum</i>	Coleochaetales	NC_004118
<i>Coleochaete scutata</i>	Coleochaetales	MK720949 *
<i>Megaceros aenigmaticus</i>	hornworts	NC_012651
<i>Phaeoceros laevis</i>	hornworts	NC_013765
<i>Aneura pinguis</i>	liverworts	NC_026901
<i>Marchantia polymorpha</i>	liverworts	NC_001660
<i>Pleurozia purpurea</i>	liverworts	NC_013444
<i>Treubia lacunosa</i>	liverworts	NC_016122
<i>Atrichum angustatum</i>	mosses	NC_024520
<i>Bartramia pomiformis</i>	mosses	NC_024519
<i>Physcomitrella patens</i>	mosses	NC_007945
<i>Sphagnum palustre</i>	mosses	NC_024521
<i>Tetraphis pellucida</i>	mosses	NC_024290
<i>Welwitschia mirabilis</i>	seed plants	NC_029130
<i>Brassica napus</i>	seed plants	NC_008285
<i>Liriodendron tulipifera</i>	seed plants	NC_021152
<i>Oryza sativa</i>	seed plants	NC_011033
<i>Cycas taitungensis</i>	seed plants	NC_010303
<i>Ginkgo biloba</i>	seed plants	NC_027976

<i>Ophioglossum californicum</i>	ferns	NC_030900
<i>Psilotum nudum</i>	ferns	NC_030952, KX171639
<i>Huperzia squarrosa</i>	lycophytes	NC_017755
<i>Isoetes engelmannii</i>	lycophytes	FJ010859, FJ176330, FJ390841, FJ536259, FJ628360

2

3

## Figure 1

A schematic representation of the topologies obtained from tree-homogeneous and tree-heterogeneous analyses of nucleotide, codon-degenerate nucleotide, and amino acid translation data.

Analyses of nucleotide data place mosses as the earliest-branching lineage of the embryophytes (1a, 1b). Analyses of codon-degenerate and amino acid data under tree-homogeneous models place liverworts as the sister-group to the remaining embryophytes (1c, 1e), whereas analyses under tree-heterogeneous models show support for the clade Setaphyta (1d, 1f).

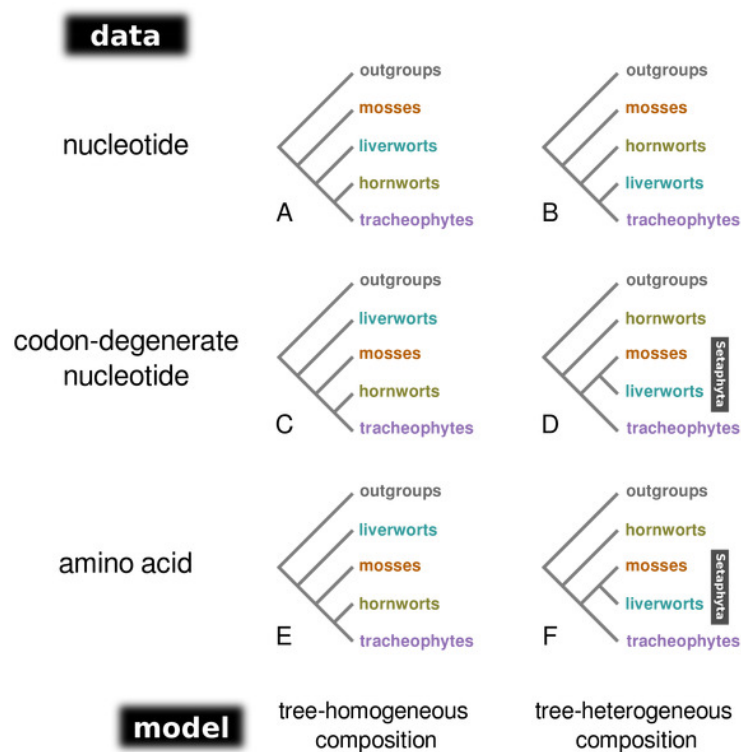


## Figure 2

Majority-rule consensus tree inferred from the 36 gene, 26 taxon concatenated amino acid data.

Bayesian MCMC with a tree-heterogeneous composition model NDCH2, marginal likelihood -  $L_h = 142829.112$ . Additional analysis statistics can be found in the legend of Fig. S7. All branches fully supported (PP=1.0). Taxa indicated as follows: outgroups, grey; hornworts, olive green; liverworts, cyan blue; mosses, orange; vascular plants, violet.

